20 Pediatric Kidney Cancer

Lisa H. Lowe and Eugenio M. Taboada

CONTENTS

20.1 Introduction

Wilms tumor is the most common solid pediatric renal neoplasm. In recent years, several less common renal malignancies that were previously considered subtypes of Wilms tumor have been recognized as separate pathological entities. Although the vast majority of pediatric renal masses are Wilms tumor, various other newly described lesions may have a particular clinical history or distinctive imaging features that differentiate them from Wilms tumor (Table 20.1); however, despite the use of modern imaging techniques, renal neoplasms cannot always be diagnosed with pre-operative imaging.

L. H. Lowe, MD, FAAP
Associate Professor of Pediatric Radiology, Children's Mercy Hospital and Clinics, University of Missouri, Kansas City, 2401 Gillham Road, Kansas City, Missouri 64108, USA
E. M. Taboada, MD, FACP
Assistant Professor of Pathology, Director of Surgical Pathology, Children's Mercy Hospital and Clinics, University of Missouri, Kansas City, 2401 Gillham Road, Kansas City, Missouri 64108, USA

This chapter reviews various renal masses in children, placing emphasis on imaging findings and clinical features that are especially useful in differentiating among renal masses. Malignant lesions are discussed first, including Wilms tumor, nephrogenic rests/nephroblastomatosis, clear cell sarcoma, rhabdoid tumor, renal cell carcinoma, renal medullary carcinoma, lymphoma, leukemia, and neuroblastoma. Benign lesions follow, with mesoblastic nephroma, ossifying renal tumor of infancy, multilocular cystic renal tumor, angiomyolipoma, and metanephric adenoma.

20.2 Wilms Tumor

Eighty-seven percent of pediatric renal masses are Wilms tumors. They occur in approximately 1:10,000 patients (Julian et al. 1995; Ritchey et al. 1995) with a peak age of presentation between 3 and 4 years (Charles et al. 1998). Eighty percent of lesions are discovered before the age of 5 years (Lonergan et al. 1998). Wilms tumors are rare in neonates, with fewer than 0.16% under 1 month of age (Charles et al. 1998; Glick et al. 2004). Bilateral masses are found in 4–13% of children (Lonergan et al. 1998), and may be associated with various congenital anomalies including cryptorchidism (2.8%), hypospadias (1.8%), hemihypertrophy (2.5%), and sporadic aniridia (White and Grossman 1991).

Genetic factors related to Wilms tumors are well documented and continue to be described and better understood (Shamberger 1999). Chromosome 11 is thought to have two loci that are implicated in the genesis of a small subset of Wilms tumors. Locus 11p13 and locus 11p15 are referred to as WT1 and WT2 genes (Lowe et al. 2000). In patients with WAGR (Wilms tumor, aniridia, genitourinary abnormalities, and mental retardation) and Drash (male pseudohermaphroditism and progressive glomeru-

Table 20.1. Age range, peak age at presentation, and distinct features of solid renal masses. *VHL* von Hippel-Lindau syndrome, *TS* tuberous sclerosis, *NF* neurofibromatosis

Renal neoplasia	Age range	Peak age	Distinct clinical and imaging features
Wilms tumor			
Unilateral	1–11 years	3.5 years	Most common solid renal mass of childhood. Most often large solid mass, often vascular invasion
Bilateral	2 months to 2 years	15 months	Associated with nephroblastomatosis and various syndromes
Nephroblastomatosis	Any age	6–18 months	Bilateral, multiple subcapsular focal masses, often with associated bilateral solid Wilms tumors
Clear cell sarcoma	1 to 4 years	2 years	Frequent skeletal metastases
Rhabdoid tumor	6 months to 9 years	6–12 months	Associated with posterior fossa cranial neoplasms
Renal cell carcinoma	6 months to 60 years	10–20 years (VHL)	Non-specific appearing mass, association with VHL
Renal medullary carcinoma	10–39 years	20 years	Exclusively seen in sickle cell trait or hemoglobin SC disease
Lymphoma			
Hodgkin disease	>10 years	Late teens	Frequently associated adenopathy but variable appearance
Non-Hodgkin lymphoma	Any age	<10 years	Bilateral renal enlargement with loss of architecture
Leukemia	Any age	Any age	Reniform, bilateral nephromegaly
Neuroblastoma	Any age	<5 years	Vascular encasement, calcification, neural extension
Mesoblastic nephroma	<1 year	1–3 months	Most common solid renal mass in infants and newborns
Ossifying renal tumor of infancy	6 days to 14 years	1–3 months	Calcified mass in an infant
Multilocular cystic renal tumor			
Cystic nephroma	3 months to 4 years	1–2 years	Large, multicystic mass in young children
Cystic partially differentiated	Adult women	Adult women	Large, multicystic mass in young women
Angiomyolipoma	6–41 years	10 years (VHL, TS, NF)	Fat and soft tissue mass associated with VHL, TS, NF
Metanephric adenoma	15 months to 83 years	None	Non-specific clinical or imaging features

lonephritis) syndromes, an abnormal WT1 gene is present, whereas patients with Beckwith-Wiedemann and hemihypertrophy have an abnormal WT2 gene. Abnormalities at other sites, including chromosomes 1, 12, and 8, have been recognized, leading to the belief that the genetics of Wilms tumor is multifactorial. Approximately 1% of Wilms tumors are familial, in which cases there is no associated anomaly of chromosome 11 (Charles et al. 1998). Children with increased risk for developing Wilms tumor should be screened starting at 6 months of age with an initial CT, followed by serial ultrasound (US) every 3–6 months until 7 years of age. Screening can be discontinued after age 7 years, since there is a significantly lower risk of developing Wilms tumor (Beckwith 1998; Lonergan et al. 1998).

Wilms tumor most commonly presents with a firm, palpable mass, but may be discovered incidentally after trauma in up to 10% of cases. Hematuria and pain are infrequent clinical findings, and constitutional symptoms are usually absent. Renin production by the tumor may cause hypertension in up to 25% of cases (Lonergan et al. 1998).

Wilms tumor originates from the metanephros (mesodermal precursors of renal parenchyma) or occasionally from mesonephric remnants within the extrarenal retroperitoneum (Shamberger 1999). Grossly, the tumor is usually a soft gray or tan mass that is sharply defined by a pseudocapsule. Varying amounts of blastema, stroma, and epithelium (triphasic) compose Wilms tumors on histological exam (Fig. 20.1). If there is differentiation along non-renal tissue lines, such as cartilage, bone, or muscle, then the mass is described histologically as "teratoid Wilms" (Fig. 20.2). Anaplasia (defined as nuclei with diameters at least three times those of adjacent cells with increased chromatin content; and multipolar or otherwise recognizable polyploid mitotic figures) is directly associated with poor response to chemotherapy and a poor prognosis (Charles et al. 1998).

Radiologically, most Wilms tumors are solid masses that distort the renal parenchyma, often with a visible pseudocapsule (Fig. 20.3). Tumor spread is usually by direct extension with displacement of adjacent structures, rather than encasement of ves-

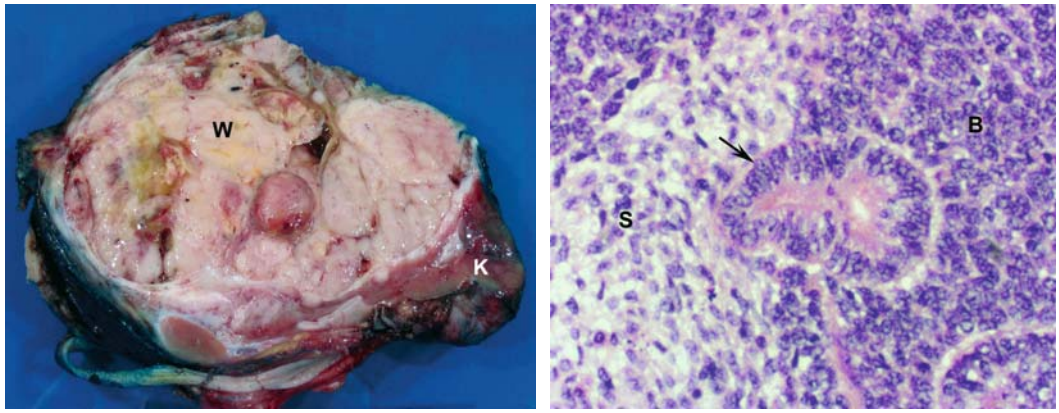

a b

Fig. 20.1a,b. Wilms tumor in a 4-year-old-boy. **a** Gross specimen reveals a pseudocapsule and septa dividing the surface of the Wilms tumor (*W*) from the kidney (*K*). **b** Histological specimen shows the "triphasic" pattern of stromal (*S*), blastemal (*B*), and tubular (*arrow*) elements.

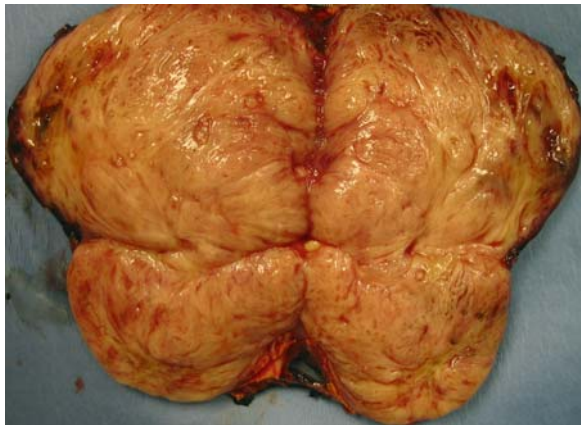

Fig. 20.2. Wilms tumor in a 4-year-old-boy. Gross specimen shows fleshy whorled surface, which on microscopy revealed heterologous tissue with abundant skeletal muscle differentiation.

Fig. 20.3. Wilms tumor in a 5-year-old boy with an abdominal mass. Axial contrast-enhanced CT scan shows a large right renal mass (*arrows*) with heterogeneous enhancement and numerous calcifications.

sels and aortic elevation, which are characteristics that suggest neuroblastoma. Formation of a tumor thrombus in the renal vein, inferior vena cava, or right atrium is typical of Wilms tumor (Fig. 20.4). Metastases to the lungs (85%), liver, and regional lymph nodes are not uncommon (Lonergan et al. 1998).

Areas of necrosis, hemorrhage, and/or calcification (9%), and the presence of adipose tissue within Wilms tumors, causes them to have heterogeneous echogenicity on US (Lonergan et al. 1998; White and Grossman 1991). Doppler interrogation of the inferior vena cava (IVC) is useful to detect vascular invasion that may modify the surgical approach. On CT Wilms tumors are heterogeneously enhancing masses with areas of calcification, fat, or lymphadenopathy. Intravenous contrast administration is essential to detect hepatic metastases, tumor thrombus, and synchronous contralateral renal masses (Lowe et al. 2000). On MR imaging, Wilms tumor is hypointense on T1- and hyperintense on T2-weighted sequences. Although MR imaging has been reported to be the most sensitive modality for determining caval patency, patients frequently require sedation during scanning. Since Wilms tumors are often very large at presentation, severe distortion of adjacent organs, including the IVC, may prohibit a determination of venous invasion/patency. In the majority of children surgical planning is possible based on meticulous US and scrutiny of multiplanar images obtained with contrast-enhanced multidetector CT. Occasionally, Wilms tumor is mostly cystic, and it is not possible to distinguish it from multilocular cystic renal tumor (Fig. 20.5).

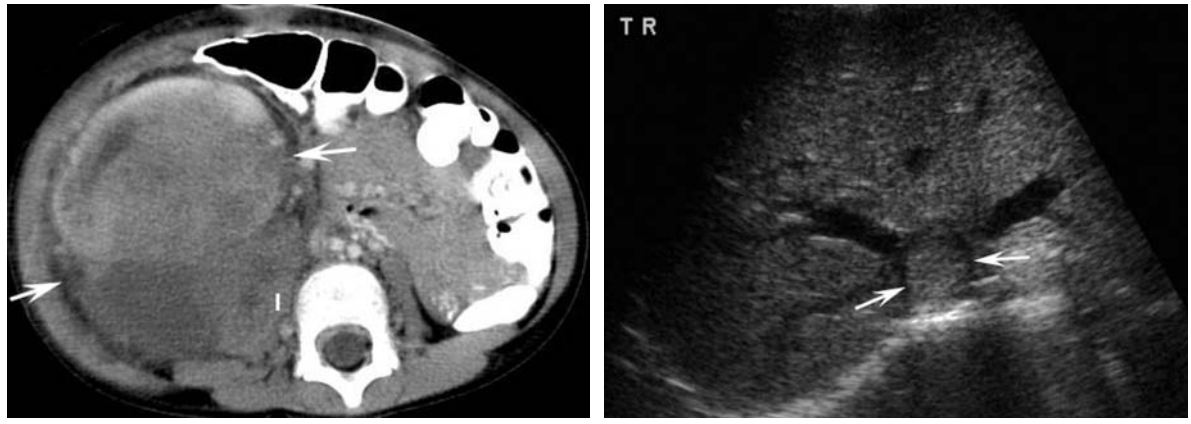

a b

Fig. 20.4a,b. Wilms tumor in a 10-year-old girl. Axial contrast-enhanced CT scan demonstrates a large right renal mass (*arrows*) with invasion of the right iliopsoas muscle (*I*). **b** Transverse US image reveals a tumor thrombus at the confluence of the hepatic veins (*arrows*).

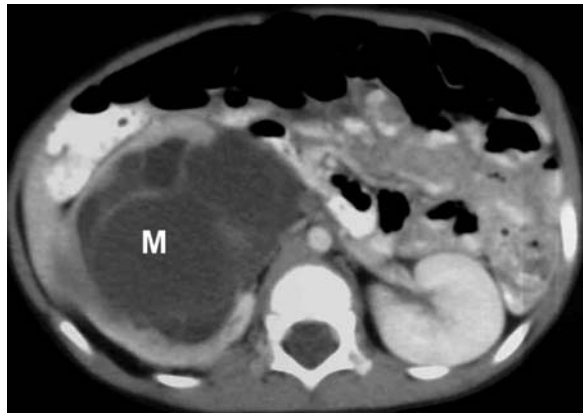

Fig. 20.5. Cystic Wilms tumor in a 3-year-old boy with an abdominal mass. Axial contrast-enhanced CT scan shows a large well-defined multiseptate cystic mass (*M*) in the right kidney. (Image courtesy of C. W. Moore)

Table 20.2. Summary of tumor prognosis

Low risk
Wilms tumor, highly epithelial type
Mesoblastic nephroma
Multilocular cystic renal tumor
Angiomyolipoma
Ossifying renal tumor of infancy
Metanephric adenoma
Intermediate risk
Wilms tumor, non-anaplastic
Neuroblastoma
Lymphoma
Leukemia
High risk
Wilms tumor, anaplastic
Renal cell carcinoma
Renal medullary carcinoma
Clear cell sarcoma
Rhabdoid tumor

Treatment of unilateral Wilms tumor includes nephrectomy and chemotherapy. In very large tumors, pre-surgical chemotherapy may promote shrinkage and improve surgical outcome. Tumor bed radiation is needed in some cases, and whole abdominal irradiation is used if there is peritoneal tumor implantation or gross tumor spillage at surgery. In bilateral Wilms tumor, each kidney is staged separately and pre-operative chemotherapy is used with the goal of complete resolution of disease in one kidney (Lowe et al. 2000). If accomplished, then nephrectomy of the contralateral kidney with eventual cure may be possible. In children with bilateral Wilms tumor in whom unilateral resolution of disease is not accomplished, the current approach is tumor resection with sparing of as much normal renal parenchyma as possible. Histology and surgical stage of disease determine the

Table 20.3. Wilms tumor staging

Stage	Description
I	Can be totally resected, limited to the kidney/renal sinus, intact renal capsule
II	Can be totally resected despite local extension beyond the kidney
III	Cannot be totally resected with residual nonhematogenous disease within the abdomen (including: residual non-resected tumor, positive margins, abdominal nodes, or contamination of the peritoneum from direct extension, implants, or spillage
IV	Hematogenous spread of disease (lung, lymph nodes, liver)
V	Bilateral masses[a]

[a]Each side should also be separately staged since prognosis is dependent on the higher individual stage

rate of cure (Tables 20.2, 20.3), which has improved from 10% in the 1920s to greater than 90% presently (Kalapurakal et al. 2004; White and Grossman 1991). Fortunately, most Wilms tumors have very favorable pathology; however, long-term follow-up is important because children treated for Wilms tumor are at an increased risk of developing secondary malignancies of the kidneys and other organ systems (Cherullo et al. 2001; Paulino et al. 2000).

20.3 Nephrogenic Rests and Nephroblastomatosis

Foci of metanephric blastema that persist in the renal parenchyma beyond 36 weeks gestation are referred to as nephrogenic rests. When diffuse or multifocal nephrogenic rests occur, the term nephroblastomatosis is applied. Although nephrogenic rests may occur incidentally in up to 1% of infants (Lonergan et al. 1998), it is currently believed that 30–40% of unilateral (Lonergan et al. 1998) and up to 99% of bilateral Wilms tumors originate from these rests (White and Grossman 1991).

Histologically, there are four types of nephrogenic rests including dormant, sclerosing, hyperplastic, or neoplastic. While dormant and sclerosing rests are usually microscopic and do not have malignant potential, hyperplastic and neoplastic rests are grossly visible and do have malignant potential (Murphy et al. 1994).

Grossly and on imaging, nephrogenic rests are classified according to location as perilobar and intralobar (Fig. 20.6; Perlman et al. 2005; Lonergan et al. 1998). This classification system is useful to the imager because it is anatomical; however, only pathological classification is able to definitively determine the lesion type and location. The term panlobar is given when there is diffuse renal involvement (Murphy et al. 1994). Perilobar rests, found in the peripheral cortex or columns of Bertin, are associated with Beckwith-Wiedemann syndrome, hemihypertrophy, Perlman syndrome (gigantism, cryptorchidism, visceromegaly, polyhydramnios, and characteristic facial features) and trisomy 18. Malignant degeneration into Wilms tumor occurs in up to 3% of patients with Beckwith-Wiedemann syndrome and hemihypertrophy (Lonergan et al. 1998). Intralobar rests are much less common, and are present in 78% of patients with Drash syndrome, nearly 100% of those with sporadic aniridia, and also occur in WAGR syndrome. Malignant degeneration is much more common with intralobar than with perilobar rests.

Fig. 20.6. Panlobar or universal nephroblastomatosis in a child. Gross specimen reveals complete loss of normal renal architecture within an extremely enlarged kidney. (With permission from Murphy et al. 1994; image courtesy of M. Rodriguez)

On US, nephrogenic rests are hypoechoic and more difficult to visualize compared with MR imaging and CT. On CT they are peripheral, hypodense, poorly enhancing nodules (Figs. 20.7, 20.8). MR imaging reveals hypointensity on T1- and T2-weighted sequences. When multiple, the nephrogenic rests of nephroblastomatosis are usually bilateral, classically subcapsular in location, and often associated with larger solid masses that indicate degeneration into Wilms tumors. With US, diffuse nephroblastomatosis causes the enlarged kidneys to be hypoechoic. Diffuse nephroblastomatosis may demonstrate a thick peripheral rind of tissue causing reniform enlargement of the kidney and a striated nephrogram after contrast administration (Lonergan et al. 1998).

The appropriate treatment for nephrogenic rests is controversial, with some authors recommending chemotherapy, whereas others maintain that close serial radiological evaluation for enlarging masses is sufficient; however, the lesions are often surgically resected since Wilms tumor must be excluded (Lonergan et al. 1998).

20.4 Clear Cell Sarcoma

Clear cell sarcoma of the kidney, also known as "bone metastasizing renal tumor of childhood," was previously considered a subtype of Wilms tumor.

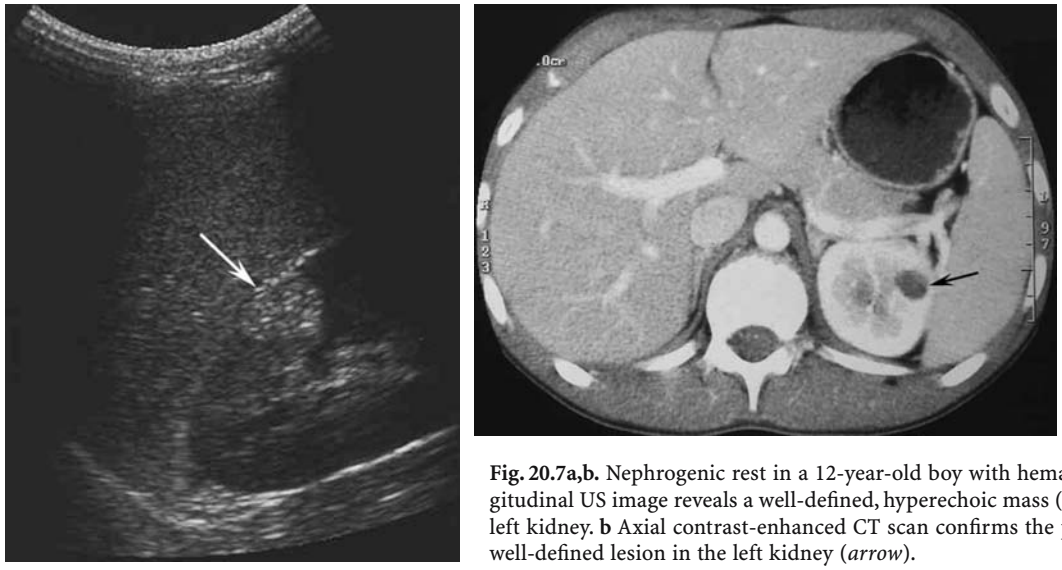

Fig. 20.7a,b. Nephrogenic rest in a 12-year-old boy with hematuria. **a** Longitudinal US image reveals a well-defined, hyperechoic mass (*arrow*) in the left kidney. **b** Axial contrast-enhanced CT scan confirms the presence of a well-defined lesion in the left kidney (*arrow*).

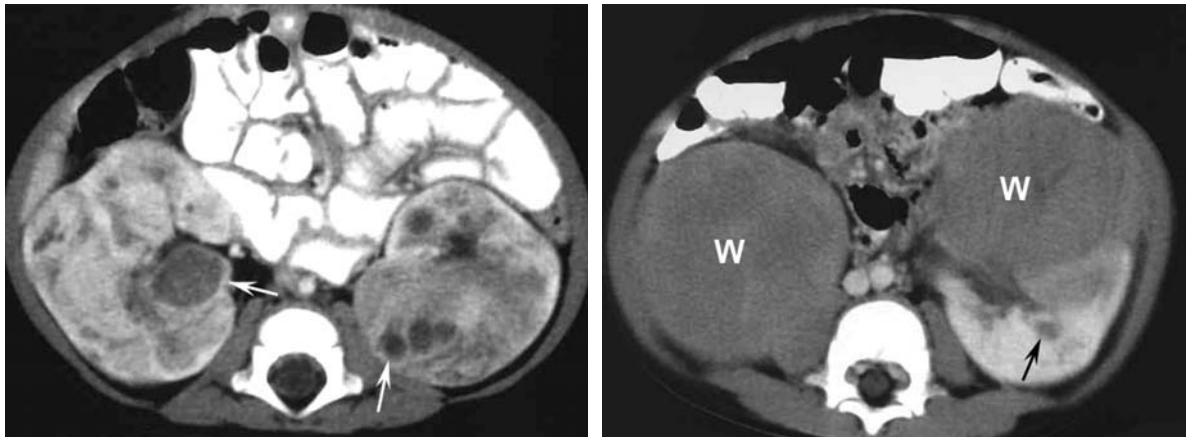

Fig. 20.8a,b. Nephroblastomatosis in a 13-month-old boy with suspected hepatosplenomegaly. **a** Axial contrast-enhanced CT scan demonstrates bilateral replacement of normal parenchyma with numerous nephrogenic rests (*arrows*), some of which are large and worrisome for developing Wilms tumor. **b** Axial contrast-enhanced CT scan of the same child 6 months later reveals progression of multiple lesions forming bilateral Wilms tumors (*W*). A focal nephrogenic rest (*arrow*) is noted.

In recent years, specific pathological features have allowed better classification of this malignancy. Clear cell sarcoma accounts for 4–5% of primary pediatric renal tumors (Charles et al. 1998; Hartman et al. 1982b) and boys are more often affected. All reported cases are unilateral and the age of peak incidence is from 1 to 4 years (Charles et al. 1998). The clinical presentation is non-specific but most often includes an abdominal mass.

Grossly, a well-circumscribed, soft mass is seen. On histological examination, small cells with inconspicuous nucleoli, ill-defined cell membranes, abundant cytoplasmic vesicles, and a prominent capillary network are characteristic (Fig. 20.9; Murphy et al. 1994); however, there is a spectrum of disease in which only 20% have clear cells.

On imaging, a well-defined, solid renal mass without intravascular extension is identified. Unfortunately, the appearance of clear cell sarcoma is nonspecific and cannot be differentiated from Wilms tumor (Fig. 20.10).

Clear cell sarcoma behaves aggressively, with a much higher rate of recurrence and mortality than Wilms tumor. It may metastasize to bone, liver, brain, lymph nodes, and lungs, in some cases long after nephrectomy. Treatment consists of chemotherapy and nephrectomy, with survival rates of up to 70% (Charles et al. 1998).

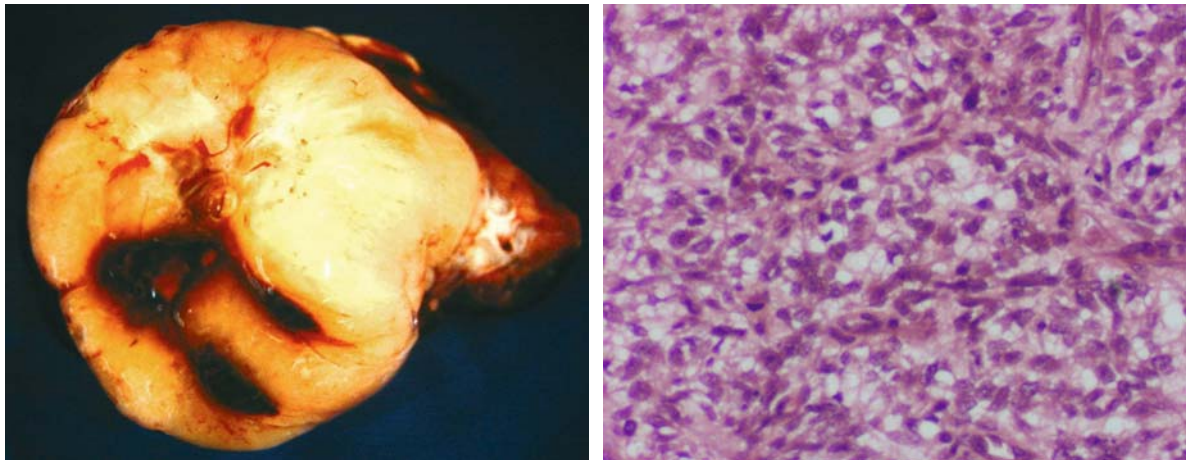

Fig. 20.9a,b. Clear cell sarcoma in a 15-month-old boy. **a** Gross specimen of a multilobulated mass. **b** Characteristic histology shows numerous cytoplasmic vesicles and delicate incomplete capillary arches. Cells contain extensive clear cytoplasm with displaced nuclei.

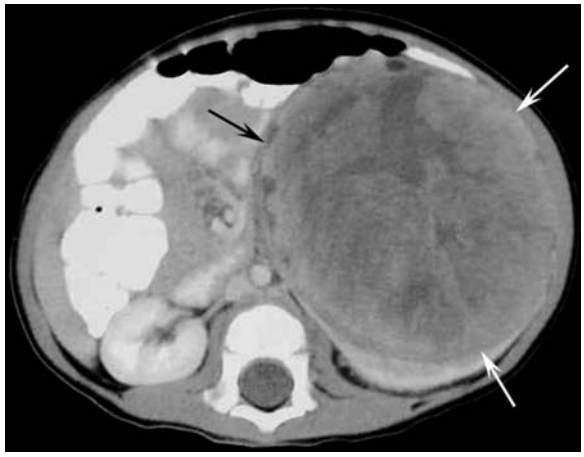

Fig. 20.10. Clear cell sarcoma in a 15-month-old boy with an abdominal mass. Axial contrast-enhanced CT scan shows a large, heterogeneously enhancing left renal mass (*arrows*).

20.5 Rhabdoid Tumor

Rhabdoid tumor, a rare, highly aggressive malignancy of early childhood, histologically resembles skeletal muscle, although a myogenic origin has not been proven. It is not related to Wilms tumor or rhabdomyosarcoma and was recently recognized as a distinct pathological entity (Lowe et al. 2000; Sacher et al. 1998). Further, recent cytogenetic studies have described a specific tumor suppressor gene on chromosome 22 in these patients. In challenging cases of rhabdoid tumor, a diagnosis is possible using cytogenetic studies, fluorescence in situ hybridization (FISH), and molecular genetic analysis (Ogino et al. 2000).

Rhabdoid tumor includes 2% of all solid pediatric renal neoplasms. There is a male predominance of 1.5:1 (Charles et al. 1998; Hartman et al. 1982b; Sacher et al. 1998). Eighty percent of cases occur at less than 2 years of age, with a median age at diagnosis of 11 months (Charles et al. 1998). Occasionally, this renal neoplasm has been reported in children up to 9 years of age. Presenting symptoms are nonspecific, but may include hematuria, an abdominal mass, or symptoms related to metastatic disease. Elevated serum calcium due to increased parathyroid hormone levels may be found. These levels normalize following tumor resection (Hartman et al. 1982b; Sacher et al. 1998).

Synchronous or metachronous primary midline posterior fossa masses or brain metastases are a well-known, unique feature of rhabdoid tumors. Specifically, ependymoma, primitive neuroectodermal tumor (PNET), and cerebellar and brain-stem astrocytoma have all been reported (Lowe et al. 2000; Sacher et al. 1998).

Grossly, rhabdoid tumors are soft, uniform, well-defined masses without a capsule (Fig. 20.11). Microscopically, monomorphous, non-cohesive cells with prominent eosinophilic nucleoli and characteristic filamentous intracytoplasmic inclusions are characteristic (Charles et al. 1998; Murphy et al. 1994). Some tumors may have superficial areas that resemble the blastemal pattern of Wilms tumor.

The imaging appearance is often indistinguishable from Wilms tumor; however, there are several characteristics that can suggest rhabdoid tumor, including subcapsular fluid collections, tumor

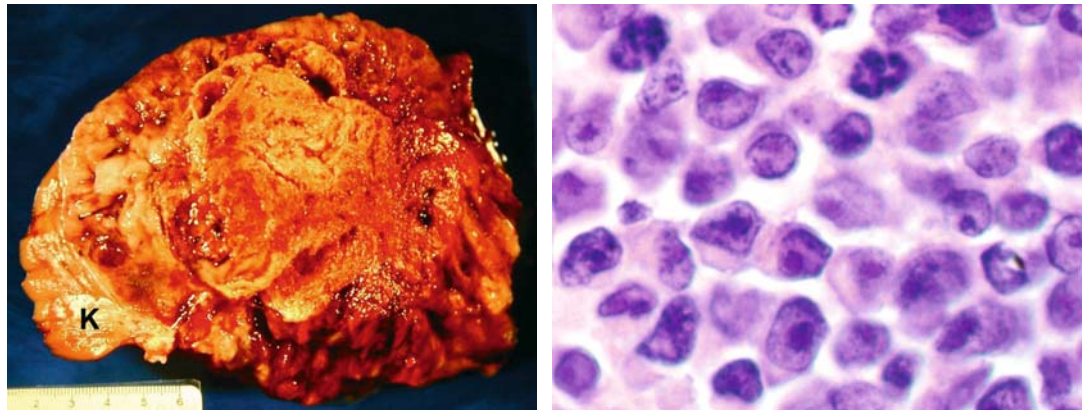

a b

Fig. 20.11a,b. Rhabdoid tumor in a 8-month-old boy. **a** Gross specimen demonstrates a pale, well-demarcated mass without a capsule. A small amount of normal kidney (*K*) is noted on the edge of the specimen. **b** Microscopic image of Rhabdoid tumor reveals monomorphic sheets of large, loosely cohesive cells with acidophilic cytoplasm, large nucleoli and distinct cell borders.

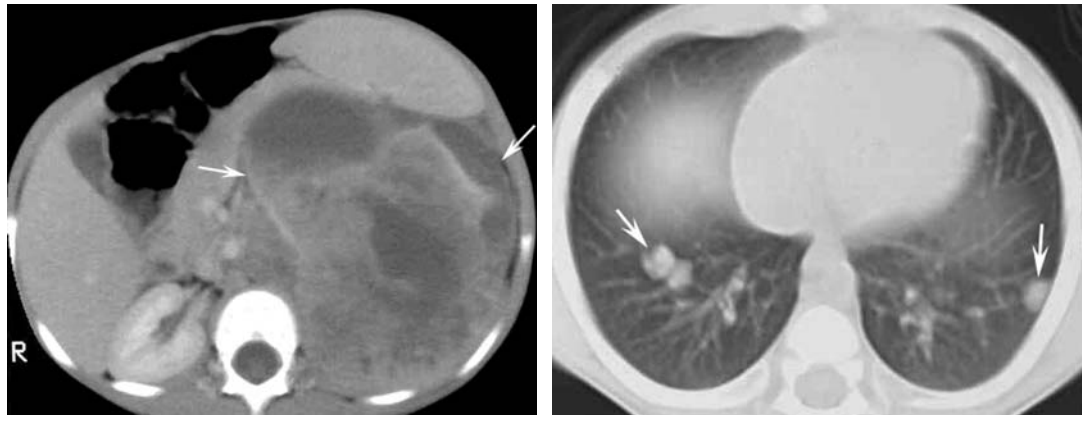

a b

Fig. 20.12a,b. Rhabdoid tumor in an 8-month-old boy with hematuria. **a** Axial contrast-enhanced CT scan demonstrates a large left renal mass (*arrows*) with heterogeneous enhancement. Noted are subcapsular fluid collections. **b** Axial CT scan through the chest identifies multiple foci of metastatic disease (*arrows*).

lobules separated by hypodense areas of necrosis or hemorrhage, and linear calcifications outlining tumor lobules (Fig. 20.12). The mass is typically large, heterogeneous, and located near or involving the renal sinus. There may be vascular and local invasion of structures (Agrons et al. 1997; Hartman et al. 1982b; Sacher et al. 1998).

Rhabdoid tumor is extremely aggressive and has a dismal prognosis with an 18-month survival rate of only 20% (Agrons et al. 1997; Charles et al. 1998; Sacher et al. 1998). Unfortunately, most children have advanced metastatic disease at the time of presentation, most commonly to the lungs (80%), and less often the liver, abdomen, brain, lymph nodes, and skeleton.

20.6 Renal Cell Carcinoma

Renal cell carcinoma (RCC) is rare in children, including less than 7% of all primary renal masses presenting at less than 20 years of age. Although Wilms tumors are 30 times more common in children than RCC (Murphy et al. 1994), they are nearly equal in incidence in the second decade (Lack et al. 1985). The vast majority of RCC occurs in adults with fewer than 2% presenting in pediatric patients. Although RCC has been reported in infants less than 6 months of age, the peak incidence occurs in the sixth decade. Patients with von Hippel-Lindau syndrome are at an increased risk of developing RCC,

in which tumors are often multiple and present at an earlier age. Because of this unique association, von Hippel-Lindau syndrome should be excluded in all children with RCC (Lack et al. 1985).

Clinically, the presentation is non-specific and the same in children as in adults. Common presenting symptoms include a palpable mass, painless gross hematuria, and flank pain. Hematuria is more common in children with RCC than those with Wilms tumor but is not useful in predicting the diagnosis or prognosis (Murphy et al. 1994).

The gross morphology of RCC is similar to that of Wilms tumor except that RCC tends to be smaller (Fig. 20.13). The normal renal architecture is usually distorted, a pseudocapsule is common, and there may be local invasion of adjacent retroperitoneal nodes. The origin of RCC remains unclear, but most authors believe that it represents an adenocarcinoma with renal tubular differentiation. Histologically, the neoplasm forms a solid infiltrative mass with variable calcification, necrosis, bleeding, and cystic degeneration (Fig. 20.14; Leuschner et al. 1991; Murphy et al. 1994). Metastases are identified at presentation in 20% of patients with the most common sites including lungs, bone, liver, and brain (Hartman et al. 1982b).

Because RCC may be somewhat small at presentation, it may be subtle on US. On CT and MR imaging, the lesion is usually easily identified as a non-specific, solid renal mass with mild contrast enhancement (Fig. 20.15). The lesion is often heterogeneous with areas of necrosis, hemorrhage, and calcification in 25% of cases (Lonergan et al. 1998). Renal cell carcinoma is treated with radical nephrectomy and regional lymphadenectomy. Unfortunately, the tumor is highly resistant to chemotherapy, making metastatic disease difficult to treat. The prognosis is mostly determined by stage at the time of presentation, with an overall survival rate of approximately 64% (Table 20.4; Geller et al. 1997).

Fig. 20.13. Renal cell carcinoma in a child. Gross specimen of clear cell type of renal cell carcinoma shows a golden color (*arrow*) due to cytoplasmic lipids. (With permission from Murphy et al. 1994)

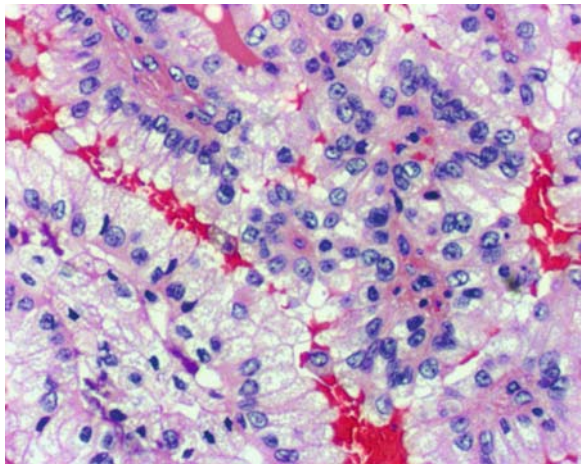

Fig. 20.14. Renal cell carcinoma in a 12-year-old boy. Histological specimen demonstrates an acinar and trabecular arrangement and clear cytoplasm.

20.7 Renal Medullary Carcinoma

Renal medullary carcinoma is a recently defined, extremely aggressive tumor occurring exclusively in teenagers and young adults with hemoglobin sickle cell (SC) disease or sickle cell trait (Davidson et al. 1995; Eble 1998). Listed as the seventh sickle cell nephropathy, the tumor does not occur in homozygous hemoglobin SS sickle cell disease (Davis et al. 1995b; Wesche et al. 1998). The mean age at presentation is 25 years (range 10–39 years). There is a male predominance (3:1) in patients under age 25 years, with an equal gender incidence over 25 years (Davis et al. 1995b). Symptoms at presentation are non-specific, including flank pain, abdominal pain, gross hematuria, weight loss, abdominal mass, and fever (Wesche et al. 1998).

Table 20.4. Renal cell carcinoma staging

Stage	Description
I	Mass <7.0 cm that is limited to the kidney
II	Mass >7.0 cm that is limited to the kidney
III	Tumor limited by Gerota's fascia (may include invasion of the ipsilateral renal vein, adrenal gland, perinephric soft tissue/fat, and/or IVC thrombus)
IV	Extension of tumor beyond Gerota's fascia

Fig. 20.15. Renal cell carcinoma in a transplanted kidney in a 12-year-old boy with suspected rejection. Axial contrast-enhanced CT scan shows multiple, well-defined foci of hypodensity within the left-lower-quadrant transplanted kidney.

The lesion arises from the epithelium at the renal pelvis–mucosa interface. Grossly, the mass fills the renal pelvis and invades adjacent vasculature and lymphatic structures (Fig. 20.16). On microscopy, drepanocytes (sickle cells), hemorrhagic foci, necrosis, stromal desmoplasia with inflammation, and a variable architectural pattern typify the lesion (Wesche et al. 1998).

Radiographically, the infiltrative, centrally located mass causes reniform enlargement with extension into the renal sinus and collecting system. Small satellite nodules and caliectasis (hydronephrosis) are typical features (Fig. 20.17). On US and CT, the lesion shows heterogeneous echogenicity and heterogeneous enhancement. In the appropriate clinical setting the differential diagnosis is limited, including transitional cell carcinoma, which is poorly documented in children, and rhabdoid tumor, which occurs in children under 3 years old (Davidson et al. 1995; Lowe et al. 2000).

The prognosis of renal medullary carcinoma is very poor, with an average survival of 15 weeks from the time of diagnosis (Davis et al. 1995b). The tumor usually presents with extensive metastatic disease, and there is a very poor response to radiotherapy and chemotherapy (Lowe et al. 2000).

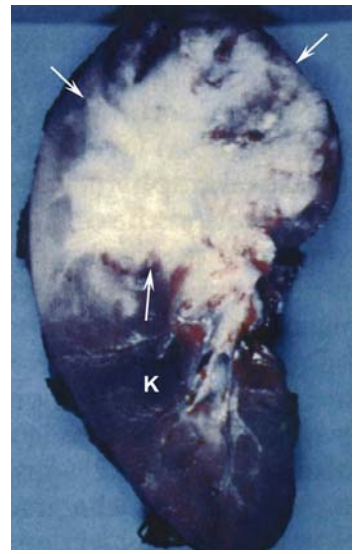

Fig. 20.16. Renal medullary carcinoma in a 16-year-old girl. Cut surface of specimen demonstrates a whorled, myomatous appearance with prominent medial extension and an ill-defined margin (*arrows*). Very little normal kidney (*K*) remains visible. (With permission from Davidson et al. 1995)

20.8 Renal Lymphoma

Renal lymphoma may be the result of direct extension from the retroperitoneum or hematogenous spread. Burkitt and non-Hodgkin lymphomas are more likely to have renal involvement in children (Chepuri et al. 2003). While less than 8% of patients with lymphoma will have their disease identified on CT, up to 62% have renal involvement on postmortem examination (Reznek et al. 1990; Sheeran and Sussman 1998). Primary renal lymphoma is disputed as an entity by most authors due to a lack of lymphatics in the kidney (Dyer et al. 1994). Primary lymphoma of the kidney has been reported only rarely and the topic remains controversial (Cohan et al. 1990). In children with lymphoma, symptoms related to the kidney usually occur late in the disease process and are non-specific, including an abdominal mass, abdominal pain, anemia, hematuria, weight loss, and occasionally hypertension (Dyer et al. 1994; Lack et al. 1985).

Imaging features vary extensively, including diffuse infiltration, focal, or multiple masses, invasion from contiguous retroperitoneal lymphadenopathy, and infrequently, perinephric disease (Fig. 20.18; Hartman et al. 1982a). Multiple focal renal nodules that variably distort the renal capsule and collecting system are the most common presenting imaging characteristics (Chepuri et al. 2003). On US, focal renal masses due to lymphoma are typically hypoechoic and may have increased through-transmission mimicking multiple cysts. The appearance on CT is non-specific. Diffuse infiltration may lead to

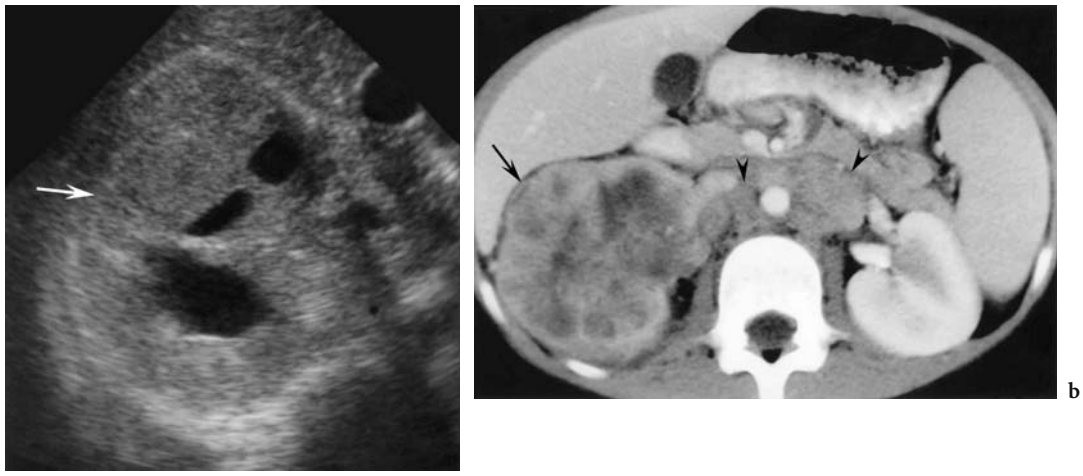

Fig. 20.17a,b. Renal medullary carcinoma in a 10-year-old boy with hematuria and sickle cell trait. **a** Transverse US image reveals loss of normal renal architecture, which is replaced by a mass (*arrow*) causing hydronephrosis. **b** Axial contrast-enhanced CT scan shows a heterogeneous mass (*arrow*) infiltrating the right kidney and adjacent retroperitoneal lymphadenopathy (*arrowheads*).

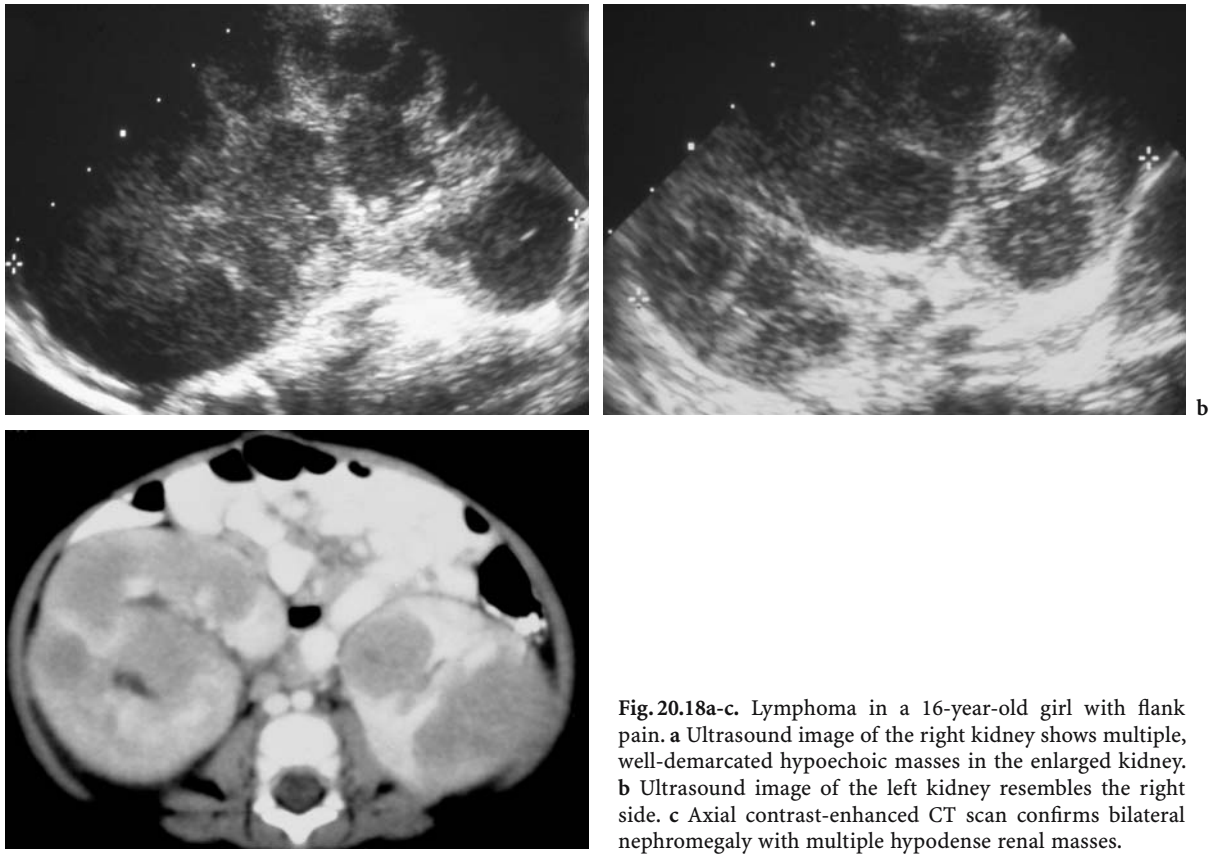

Fig. 20.18a-c. Lymphoma in a 16-year-old girl with flank pain. **a** Ultrasound image of the right kidney shows multiple, well-demarcated hypoechoic masses in the enlarged kidney. **b** Ultrasound image of the left kidney resembles the right side. **c** Axial contrast-enhanced CT scan confirms bilateral nephromegaly with multiple hypodense renal masses.

reniform enlargement, retroperitoneal disease may cause ureteral or vascular encasement, and perinephric spread may be the result of direct retroperitoneal extension or intraparenchymal invasion through the renal capsule (Chepuri et al. 2003). Focal lesions are generally homogeneous and hypodense both before and after contrast administration with some cases simulating the appearance of multiple renal cysts (Capps and Das Narla 1995). Perinephric spread may be identified as soft tissue nodules, focal curvilinear densities, thickening of the renal capsule/Gerota's fascia, or direct invasion from retroperitoneal nodes (Dyer et al. 1994). Perirenal lymphoma without renal parenchymal disease is rare, but unusual in appearance on CT (Hartman et al. 1982a) where it manifests as a hypodense soft tissue plaque encasing the kidney (Sheeran and Sussman 1998). Angiography is no longer performed but has been reported to show hypovascular foci.

Prognosis in patients with lymphoma is unrelated to the presence of renal involvement (Chepuri et al. 2003).

20.9 Leukemia

Leukemic (acute and chronic, myelogenous and lymphoblastic) involvement of the kidneys is common during the hematologically active stage of disease (Butani and Paulson 2003). The kidneys may act as a sanctuary for residual disease during remission. Clinically, symptoms related to renal leukemia are unusual but may include renal failure or hypertension. Grossly, leukemia infiltrates the kidneys causing reniform enlargement.

Imaging features are variable but may include unilateral or bilateral nephromegaly, hydronephrosis, altered architecture, abnormal echogenicity on US, and poor contrast excretion on CT (Butani and Paulson 2003).

20.10 Neuroblastoma

Neuroblastoma is the most common tumor of early childhood, occurring most often in children under age 5 years (David et al. 1989; Kushner 2004). It originates from the neural crest cells and arises most often from the adrenal medulla but may occur anywhere along the sympathetic chain from the skull base to the pelvis (Mehta et al. 2003). The presentation varies, ranging from a palpable abdominal mass, to various paraneoplastic syndromes, or symptoms related to metastatic disease (David et al. 1989; Matthay et al. 2003; Mehta et al. 2003). The diagnosis is often made by analysis of urinary catecholamines, or from bone marrow aspirates (Kushner 2004). The kidney is most often involved by invasion from an adjacent adrenal primary, or direct extension of retroperitoneal disease.

Imaging features include a solid mass with calcifications on plain radiographs and a heterogeneous mostly hyperechoic mass on US. Vascular encasement and calcification by a large, heterogeneously enhancing mass is seen on CT (Fig. 20.19). Metastatic disease is commonly detected at presentation by bone marrow aspirate, bone scan, I-131 metaiodobenzylmandelic scintigraphy (MIBG), and CT (Matthay et al. 2003; Mehta et al. 2003). In general, the prognosis is better with younger age, lower grade, lower stage, and n-myc amplification (Moore et al. 2004).

20.11 Mesoblastic Nephroma

Mesoblastic nephroma, also referred to as fetal renal hamartoma or leiomyomatous hamartoma, was originally thought to represent congenital Wilms tumor

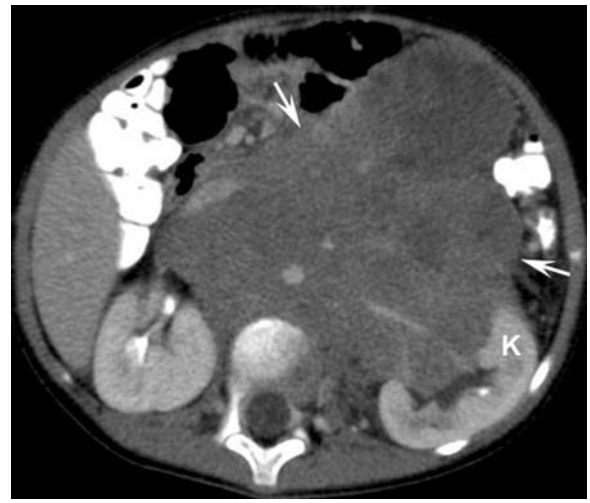

Fig. 20.19. Neuroblastoma in a 5-year-old boy with a palpable mass. Axial contrast-enhanced CT scan shows a soft tissue mass (*arrows*) centered within the retroperitoneum and extending into the left renal sinus abutting the kidney (*K*).

but is now recognized as a distinct entity. Mesoblastic nephroma is by far the most common solid renal mass in neonates (Donaldson and Shkolnik 1988; Glick et al. 2004). It is slightly more common in boys and usually presents at under 3 months of age, with 90% of lesions discovered by 12 months of age (Glick et al. 2004; Hartman et al. 1982b; Lowe et al. 2000). The clinical presentation is most often a palpable abdominal mass or less frequently hematuria. Cases are increasingly detected with prenatal US. An association with hydrops, polyhydramnios, increased renin levels, and premature delivery has been described (Glick et al. 2004).

Pathologically, mesoblastic nephroma is believed to be due to early proliferation of nephrogenic mesenchyme. On gross pathology, the tumor is usually large, rubbery, infiltrative, poorly defined, and without a capsule (Fig. 20.20). Histologically, the tumors are "monomorphic," with infiltrating finger-like projections of spindled mesenchymal cells and embryonal metaplasia of entrapped renal tissue (Charles et al. 1998; Hartman et al. 1982b).

Radiological studies demonstrate a solid intrarenal mass that often extends into the renal sinus and may have focal perinephric space infiltration. A large portion of the renal parenchyma may be replaced by the mass, which may be hemorrhagic, necrotic, or partially cystic (Fig. 20.21).

Mesoblastic nephroma is usually benign and is treated with nephrectomy (Julian et al. 1995). A wide surgical margin is necessary due to the infiltrative nature of the lesion which may recur locally if incompletely resected. Occasionally, metastases to lung, brain, or bones are reported. It is recommended that patients be followed closely for 1 year after surgical resection since histological characteristics cannot reliably predict biological behavior (Charles et al. 1998; Leuschner et al. 1991). When mesoblastic nephroma is found and resected early (at <6 months of age), the prognosis is excellent (Lowe et al. 2000).

Fig. 20.20. Mesoblastic nephroma in an infant. Gross specimen shows classic whorled, myxomatous infiltrative mass with poor demarcation from the normal renal parenchyma. (With permission from Murphy et al. 1994)

20.12 Ossifying Renal Tumor of Infancy

Ossifying renal tumor of infancy (ORTI) is a rare, benign renal mass first described in 1980

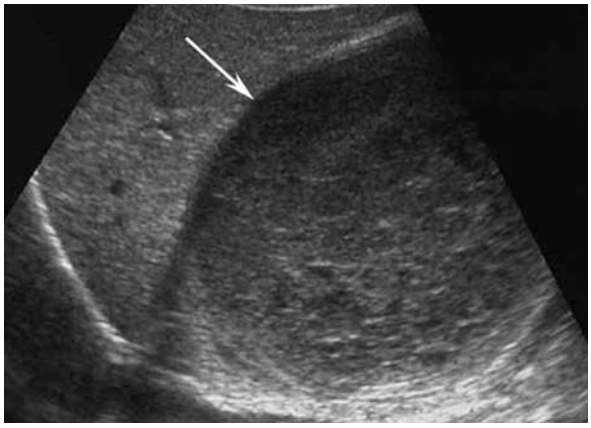

a

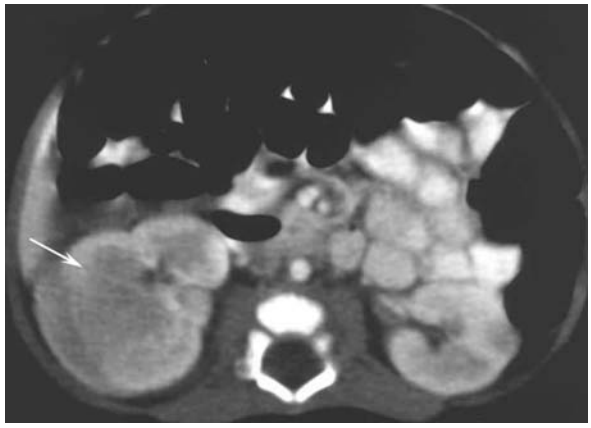

b

Fig. 20.21a,b. Mesoblastic nephroma in a 5-week-old infant with an in utero renal mass. **a** Longitudinal US image reveals a mixed echo texture mass (*arrow*) replacing most of the right kidney. **b** Axial contrast-enhanced CT scan reveals a hypodense, ill-defined, infiltrative, right renal mass (*arrow*).

(Chatten et al. 1980). Since then, only 11 cases have been reported in children with an age range of 6 days to 14 months (Chatten et al. 1980; Glick et al. 2004; Sotelo-Avila et al. 1995; Vazquez et al. 1998). ORTI is more common in boys (8 of 11), more common on the left side (9 of 11), and hematuria was the presenting symptom in 10 of 11 children. The upper pole calyces were involved in 7 of 11 cases (Sotelo-Avila et al. 1995).

ORTI is a urothelial lesion originating from the papillary portion of the renal pyramid. The lesion enlarges in a polypoid fashion, extending into the collecting system and usually reaching a size of no more than 2–3 cm.

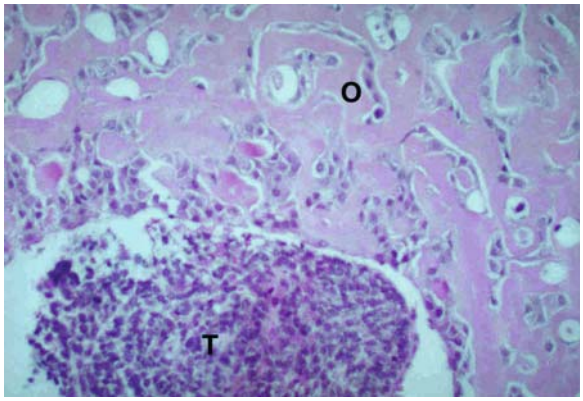

Fig. 20.22. Ossifying renal tumor of infancy in a child. Microscopic specimen reveals an osteoid core (*O*) with peripheral tubules (*T*) and mesenchyme/fibrous connective tissue. (With permission from Lowe et al. 2000)

Three basic histological components are found within the lesion: the osteoid core; osteoblasts; and spindle cells. In relatively older children, mature osteoid elements tend to be more prominent (Fig. 20.22). It is believed by some authors that the osteoid elements within the lesion are the result of urothelial cells with osteogenic potential (Chatten et al. 1980; Davis et al. 1995b). Other investigators hypothesize that spindle cells within the tumor resemble intralobular nephrogenic rests, thus indicating a mass in the pathological spectrum of Wilms tumor. Despite these two theories, Wilms tumor has never been reported in association with any of these children.

Imaging studies of ORTI typically show a calcified mass causing a filling defect and partial obstruction of the collecting system (Lowe et al. 2000). The appearance may resemble a staghorn calculus, which is not a differential consideration in a child of this age (Vazquez et al. 1998). Calcifications are present within 9 of 11 cases of ORTI with only the two youngest patients having no calcifications (Sotelo-Avila et al. 1995). Specific findings by modality include an echogenic shadowing mass with or without hydronephrosis on US, and a smoothly demarcated, poorly enhancing, calcified mass on CT (Fig. 20.23).

The prognosis of ORTI is excellent with no reports of metastatic disease or recurrence after surgical resection. Follow-up of the disease-free state has been documented from 4 months up to 23 years (Ito et al. 1998).

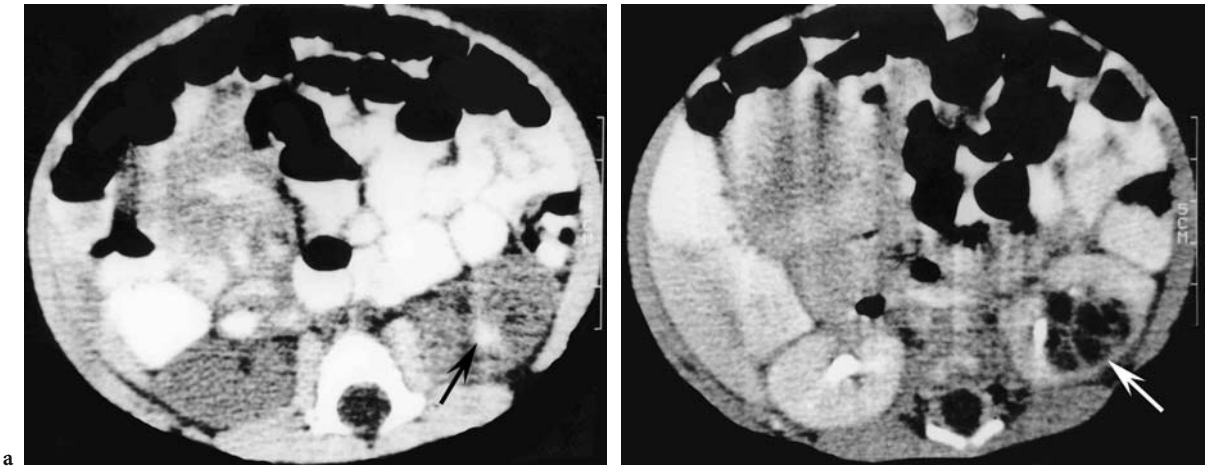

Fig. 20.23a,b. Ossifying renal tumor of infancy in a 2-month-old boy with an abdominal mass. **a** Axial unenhanced CT scan reveals a calcification (*arrow*) within the left kidney. **b** After contrast administration, axial CT scan demonstrates a hypodense mass (*arrow*) with septations. (With permission from Lowe et al. 2000)

20.13 Multilocular Cystic Renal Tumor

The term multilocular cystic renal tumor includes a group of uncommon, benign cystic renal lesions that are indistinguishable grossly and radiologically (Agrons et al. 1995; Charles et al. 1998). These masses range from purely cystic (cystic nephroma, CN), epithelial lined with fibrous septa to a mass with mature tubules and septa containing foci of blastemal cells (cystic partially differentiated nephroblastoma, CPDN; Ferrer and McKenna 1994; Shamberger 1999). Septations within the CPDN form the only solid portions of the tumor (Fig. 20.24). Cystic Wilms tumor is distinguished from CPDN by the presence of expansile solid masses of nephroblastomatous tissue.

Two distinct peak ages of incidence occur in multilocular cystic renal tumors. The first occurs in boys 3 months to 4 years, typically CN, and the second occurs in adult women, typically CPDN (Lonergan et al. 1998). The presentation is non-specific with a painless abdominal mass and occasional systemic symptoms (Sacher et al. 1998).

Cross-sectional imaging with US, CT, or MR imaging reveals a well-defined, cystic mass with enhancing septa. The cysts range in size from a few millimeters up to 4 cm, and the amount of enhancing septa determines the degree to which the lesion may appear more or less solid (Fig. 20.25). A capsule may be present and extracapsular extension may occur.

Multilocular cystic renal tumors are treated by complete surgical resection and have an excellent prognosis. Occasionally, chemotherapy or local radiation is required to treat tumor recurrence; however, there are no reports of metastatic disease (Gonzalez-Crussi et al. 1982).

20.14 Angiomyolipoma

Angiomyolipoma is a benign hamartomatous neoplasm consisting of disordered fat, smooth muscle, and vascular tissue (Chung et al. 1998; Eble 1998; Ewalt et al. 1998). It is almost always associated with tuberous sclerosis in children (Eble 1998; Lowe et al. 2000), but overall is most often sporadic (Lemaitre et al. 1995). By the age of 10 years, 80% of children with tuberous sclerosis will have angiomyolipomas (Chung et al. 1998). Other associations with angiomyolipoma include neurofibromatosis and von Hippel-Lindau syndrome. Women are affected 4:1 compared with men, and the average age at presentation for all cases is 41 years. Angiomyolipomas are typically multifocal, bilateral, and often large in size.

Lesions less than 4 cm in size are generally asymptomatic; however, larger lesions may present with symptoms such as flank pain, abdominal pain, hematuria, or severe hemorrhage (Ewalt et al. 1998; Hartman et al. 1982b). Hemorrhage within angiomyolipomas is believed secondary to bleeding aneurysms within the abundant abnormal, elastin-poor vascularity of the tumor (Eble 1998). "Wunderlich syndrome," or severe retroperitoneal hemorrhage, has been described in larger lesions and may be life-threatening (Hennigar and Beckwith 1992).

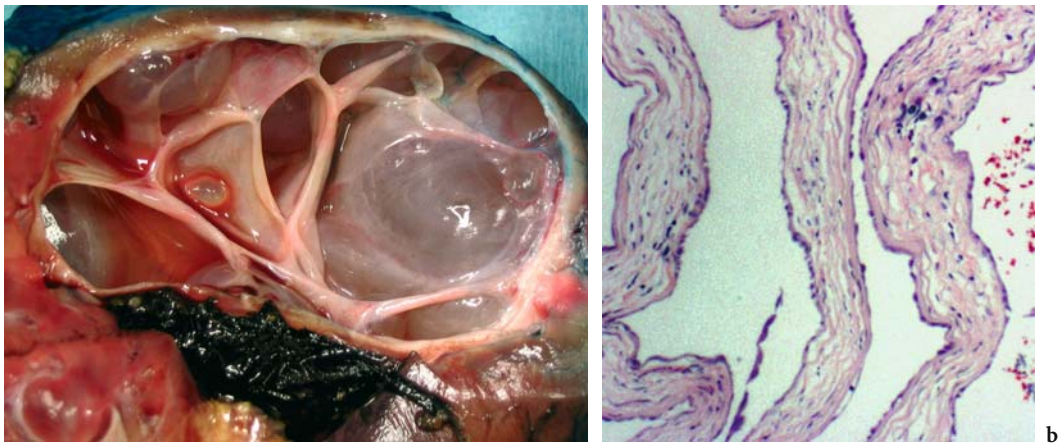

Fig. 20.24a,b. Cystic nephroma in a 2-year-old boy. **a** Gross appearance of cystic mass with well-defined, smooth margins, and multiple septations. **b** Microscopic image shows fibrous tissue in the walls of the cysts without the presence of other nephroblastic elements.

Fig. 20.25. Cystic nephroma in a 2-year-old boy with an abdominal mass on a well-child visit to the pediatrician. Coronal reconstructed contrast-enhanced CT image demonstrates a large septate right renal mass (*arrows*).

The radiological appearance of angiomyolipoma varies depending on the presence or absence of tissue components. Ultrasound reveals hyperechoic non-shadowing foci in fatty regions, iso- to hypoechoic foci in regions of soft tissue, and hypervascularity regions on color Doppler evaluation. The imaging diagnosis is often specific if fat is found in the mass on CT or MR imaging (Fig. 20.26). Catheter angiography may show characteristic dilated tortuous vessels with aneurysm formation but is not generally indicated for diagnosis. It may be necessary if intervention is required for temporization of severe bleeding. The differential diagnosis of angiomyolipoma includes Wilms tumor and renal cell carcinoma, both of which may also contain fat; however, in the appropriate clinical setting and with typical imaging features, a specific diagnosis of angiomyolipoma is usually not problematic. Although angiomyolipoma is a benign lesion, it may rarely invade neighboring structures such as lymph nodes or the inferior vena cava (Lowe et al. 2000).

Because there is a high rate of angiomyolipomas in patients with tuberous sclerosis, screening US is recommended every 2–3 years before puberty and every year thereafter to check for growing lesions (Chung et al. 1998). In children with lesions larger than 4 cm, prophylactic partial nephrectomy, or selective catheter embolization may be considered to avoid potentially life-threatening bleeding (Hartman et al. 1982b). Unfortunately, in children with tuberous sclerosis there is often replacement of a majority of normal renal parenchyma by cysts and angiomyolipomas that ultimately results in end-stage renal disease, and in these children, preservation of functional renal tissue becomes the priority.

20.15 Metanephric Adenoma

Metanephric adenoma is also known as embryonal adenoma, or nephrogenic adenofibroma (Ito et al. 1998; Navarro et al. 1999). It is a benign unilateral mass that is more common in women and has been reported from age 15 months to 83 years (Davis et al. 1995a). Presenting features include an abdominal mass, hypertension, abdominal pain, hypercalcemia, hematoma, and polycythemia. The gross appearance is non-specific, and microscopically numerous psammoma bodies can be identified among spindled mesenchymal cells that surround nodules of embryonal epithelium (Fig. 20.27; Murphy et al. 1994; Navarro et al. 1999).

Imaging features are non-specific and include a well-defined, solid lesion on US that is hypovascular with Doppler, with possible cystic change or a mural nodule (Mahoney et al. 1997). Unenhanced CT images reveal a hyper- or isodense mass that may contain small calcifications (Davis et al. 1995a; Navarro et al. 1999). After contrast administration the mass is hypodense compared with normal renal tissue (Fig. 20.28; Chefchaouni et al. 1996).

Because metanephric adenoma is a benign lesion treated with local surgical excision and normal renal parenchymal sparing, it is important to include it in

Fig. 20.26. Angiomyolipomas in a 17-year-old girl with tuberous sclerosis. Axial contrast-enhanced CT scan reveals bilateral heterogeneous enhancement of multiple renal masses containing soft tissue and fat components. Subtle, tiny peripheral renal cortical cysts are also noted.

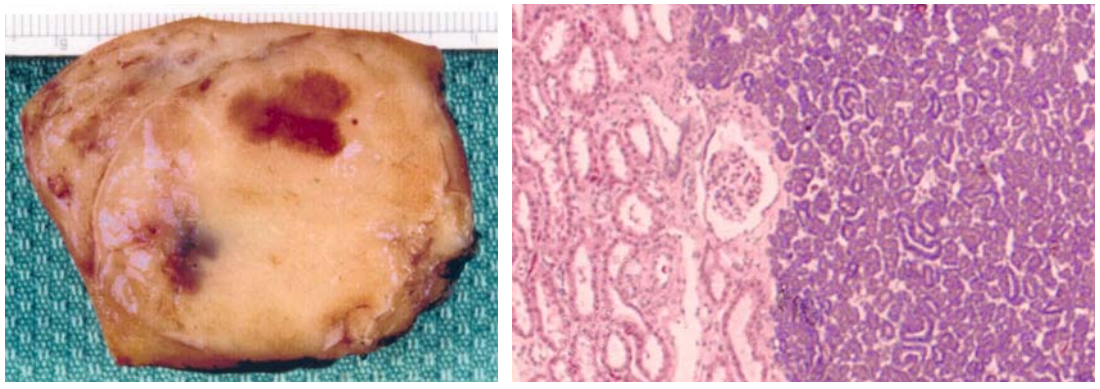

Fig. 20.27a,b. Metanephric adenoma in a 9-year-old girl. **a** Gross cut surface of mass demonstrates focus of hemorrhage without necrosis. **b** Histological specimen shows tubular and acinar structures adjacent to normal kidney on the left. Nuclei are homogenous and bland without mitotic activity (hematoxylin and eosin stain; original magnification, ×50). (With permission from Navarro et al. 1999; image courtesy of G. Taylor)

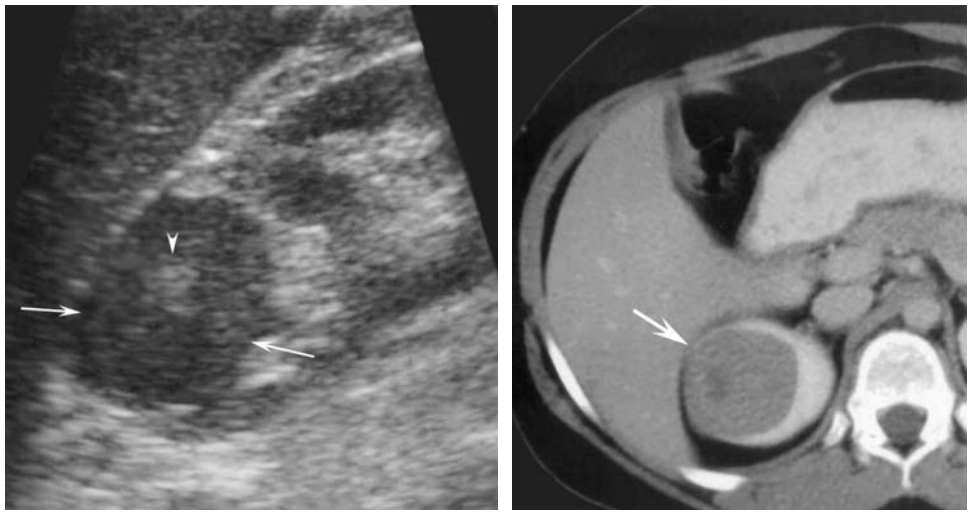

Fig. 20.28a,b. Metanephric adenoma in a 9-year-old girl with three episodes of urinary tract infection. **a** Longitudinal US image demonstrates a well-defined, hypoechoic mass (*arrows*) in the right kidney with a central focus of hyperechogenicity (*arrowhead*). **b** Axial contrast-enhanced CT scan reveals homogeneous, mildly enhancing mass (*arrow*) in the right kidney. (With permission from Navarro et al. 1999)

the differential diagnosis of pediatric renal masses (Murphy et al. 1994; Navarro et al. 1999).

20.16 Conclusion

In conclusion, Wilms tumor is characterized by displacement of structures, vascular invasion, and bilaterality in 10% of cases. Nephrogenic rests and nephroblastomatosis occur most often in neonates, and are distinguished by multiple, bilateral, subcapsular masses, and associated Wilms tumors. Frequent skeletal metastases suggest clear cell sarcoma and a synchronous posterior fossa mass suggests rhabdoid tumor. Pediatric renal cell carcinoma occurs in the second decade and is associated with von Hippel-Lindau disease. Renal medullary carcinoma is a highly aggressive tumor seen exclusively in teenagers and young adults with sickle cell trait or SC disease. The appearance of renal lymphoma is variable, but most often includes multiple homogeneous masses with retroperitoneal lymphadenopathy. Leukemic infiltration of the kidneys causes bilateral reniform enlargement, although the diagnosis is usually not a dilemma based on the clinical history. Neuroblastoma is distinguished by direct

extension of a retroperitoneal mass with vascular encasement and often has calcifications.

The primary differential diagnosis in a neonate with a solid renal mass is mesoblastic nephroma. Differentiation of ossifying renal tumor in infancy is possible by the presence of ossified elements. A large renal mass with multiple cysts and little solid tissue raises concern for multilocular cystic renal tumor. Angiomyolipomas contain fat and soft tissue, are often multiple and in children predominantly occur in association with tuberous sclerosis. Metanephric adenoma lacks specific features but is always well defined.

References

Agrons GA, Wagner BJ, Davidson AJ, Suarez ES (1995) Multilocular cystic renal tumor in children: radiologic–pathologic correlation. Radiographics 15:653–669

Agrons GA, Kingsman KD, Wagner BJ, Sotelo-Avila C (1997) Rhabdoid tumor of the kidney in children: a comparative study of 21 cases. Am J Roentgenol 168:447–451

Beckwith JB (1998) Children at increased risk for Wilms tumor: monitoring issues. J Pediatr 132:377–379

Butani L, Paulson TE (2003) Congenital acute myelogenous leukemia presenting as palpable renal masses in a neonate. J Pediatr Hematol Oncol 25:240–242

Capps GW, Das Narla L (1995) Renal lymphoma mimicking clear cell sarcoma in a pediatric patient. Pediatr Radiol 25 (Suppl 1):S87–S89

Charles AK, Vujanic GM, Berry PJ (1998) Renal tumours of childhood. Histopathology 32:293–309

Chatten J, Cromie WJ, Duckett JW (1980) Ossifying tumor of infantile kidney: report of two cases. Cancer 45:609–612

Chefchaouni MC, Zerbib M, Homsi T, Saighi D, Flam T, Thiounn N, Debre B (1996) Metanephric adenoma: an unusual tumor of the kidney. Apropos of a case. J Urol (Paris) 102:40–43

Chepuri NB, Strouse PJ, Yanik GA (2003) CT of renal lymphoma in children. Am J Roentgenol 180:429–431

Cherullo EE, Ross JH, Kay R, Novick AC (2001) Renal neoplasms in adult survivors of childhood Wilms tumor. J Urol 165:2013–2017

Chung CJ, Fordham L, Little S, Rayder S, Nimkin K, Kleinman PK, Watson C (1998) Intraperitoneal rhabdomyosarcoma in children: incidence and imaging characteristics on CT. Am J Roentgenol 170:1385–1387

Cohan RH, Dunnick NR, Leder RA, Baker ME (1990) Computed tomography of renal lymphoma. J Comput Assist Tomogr 14:933–938

David R, Lamki N, Fan S, Singleton EB, Eftekhari F, Shirkhoda A, Kumar R, Madewell JE (1989) The many faces of neuroblastoma. Radiographics 9:859–882

Davidson AJ, Choyke PL, Hartman DS, Davis CJ Jr (1995) Renal medullary carcinoma associated with sickle cell trait: radiologic findings. Radiology 195:83–85

Davis CJ Jr, Barton JH, Sesterhenn IA, Mostofi FK (1995a) Metanephric adenoma: clinicopathological study of fifty patients. Am J Surg Pathol 19:1101–1114

Davis CJ Jr, Mostofi FK, Sesterhenn IA (1995b) Renal medullary carcinoma. The seventh sickle cell nephropathy. Am J Surg Pathol 19:1–11

Donaldson JS, Shkolnik A (1988) Pediatric renal masses. Semin Roentgenol 23:194–204

Dyer RB, Lowe LH, Zagoria RJ, Amis ES Jr (1994) Mass effect in the renal sinus: an anatomic classification. Curr Probl Diagn Radiol 23:1–27

Eble JN (1998) Angiomyolipoma of kidney. Semin Diagn Pathol 15:21–40

Ewalt DH, Sheffield E, Sparagana SP, Delgado MR, Roach ES (1998) Renal lesion growth in children with tuberous sclerosis complex. J Urol 160:141–145

Ferrer FA, McKenna PH (1994) Partial nephrectomy in a metachronous multilocular cyst of the kidney (cystic nephroma). J Urol 151:1358–1360

Geller E, Smergel EM, Lowry PA (1997) Renal neoplasms of childhood. Radiol Clin North Am 35:1391–1413

Glick RD, Hicks MJ, Nuchtern JG, Wesson DE, Olutoye OO, Cass DL (2004) Renal tumors in infants less than 6 months of age. J Pediatr Surg 39:522–525

Gonzalez-Crussi F, Kidd JM, Hernandez RJ (1982) Cystic nephroma: morphologic spectrum and implications. Urology 20:88–93

Hartman DS, David CJ Jr, Goldman SM, Friedman AC, Fritzsche P (1982a) Renal lymphoma: radiologic–pathologic correlation of 21 cases. Radiology 144:759–766

Hartman DS, Davis CJ Jr, Madewell JE, Friedman AC (1982b) Primary malignant renal tumors in the second decade of life: Wilms tumor versus renal cell carcinoma. J Urol 127:888–891

Hennigar RA, Beckwith JB (1992) Nephrogenic adenofibroma. A novel kidney tumor of young people. Am J Surg Pathol 16:325–334

Ito J, Shinohara N, Koyanagi T, Hanioka K (1998) Ossifying renal tumor of infancy: the first Japanese case with long-term follow-up. Pathol Int 48:151–159

Julian JC, Merguerian PA, Shortliffe LM (1995) Pediatric genitourinary tumors. Curr Opin Oncol 7:265–274

Kalapurakal JA, Dome JS, Perlman EJ, Malogolowkin M, Haase GM, Grundy P, Coppes MJ (2005) Management of Wilms' tumour: current practice and future goals. Lancet Oncol 5:37-46

Kushner BH (2004) Neuroblastoma: a disease requiring a multitude of imaging studies. J Nucl Med 45:1172–1188

Lack EE, Cassady JR, Sallan SE (1985) Renal cell carcinoma in childhood and adolescence: a clinical and pathological study of 17 cases. J Urol 133:822–828

Lemaitre L, Robert Y, Dubrulle F, Claudon M, Duhamel A, Danjou P, Mazeman E (1995) Renal angiomyolipoma: growth followed up with CT and/or US. Radiology 197:598–602

Leuschner I, Harms D, Schmidt D (1991) Renal cell carcinoma in children: histology, immunohistochemistry, and follow-up of 10 cases. Med Pediatr Oncol 19:33–41

Lonergan GJ, Martinez-Leon MI, Agrons GA, Montemarano H, Suarez ES (1998) Nephrogenic rests, nephroblastomatosis, and associated lesions of the kidney. Radiographics 18:947–968

Lowe LH, Isuani BH, Heller RM, Stein SM, Johnson JE, Navarro OM, Hernanz-Schulman M (2000) Pediatric renal masses: Wilms tumor and beyond. Radiographics 20:1585–1603

Mahoney CP, Cassady C, Weinberger E, Winters WD, Benjamin DR (1997) Humoral hypercalcemia due to an occult renal adenoma. Pediatr Nephrol 11:339–342

Matthay KK, Brisse H, Couanet D, Couturier J, Benard J, Mosseri V, Edeline V, Lumbroso J, Valteau-Couanet D, Michon J (2003) Central nervous system metastases in neuroblastoma: radiologic, clinical, and biologic features in 23 patients. Cancer 98:155–165

Mehta K, Haller JO, Legasto AC (2003) Imaging neuroblastoma in children. Crit Rev Comput Tomogr 44:47–61

Moore SW, Satge D, Sasco AI (2004) The epidemiology of neonatal tumors. J Pediatr Surg 39:1150–1151

Murphy WM, Beckwith JB, Farrow GM (1994) Tumors of the kidney, bladder, and related urinary structures. Armed Forces Institute of Pathology, Washington, DC

Navarro O, Conolly B, Taylor G, Bagli DJ (1999) Metanephric adenoma of the kidney: a case report. Pediatr Radiol 29:100–103

Ogino S, Ro TY, Redline RW (2000) Malignant rhabdoid tumor: A phenotype? An entity?--A controversy revisited. Adv Anat Pathol 7:181-190

Paulino AC, Wen BC, Brown CK, Tannous R, Mayr NA, Zhen WK, Weidner GJ, Hussey DH (2000) Late effects in children treated with radiation therapy for Wilms' tumor. Int J Radiat Oncol Biol Phys 46:1239–1246

Perlman EJ, Faria P, Soares A, Hoffer F, Sredni S, Ritchey M, Shamberger RC, Green D, Beckwith JB (2005) Hyperplastic perilobar nephroblastomatosis: Long-term survival of 52 patients. Pediatr Blood Cancer Apr 6; [Epub ahead of print]

Reznek RH, Mootoosamy I, Webb JA, Richards MA (1990) CT in renal and perirenal lymphoma: a further look. Clin Radiol 42:233–238

Ritchey ML, Azizkhan RG, Beckwith JB, Hrabovsky EE, Haase GM (1995) Neonatal Wilms tumor. J Pediatr Surg 30:856–859

Sacher P, Willi UV, Niggli F, Stallmach T (1998) Cystic nephroma: a rare benign renal tumor. Pediatr Surg Int 13:197–199

Shamberger RC (1999) Pediatric renal tumors. Semin Surg Oncol 16:105–120

Sheeran SR, Sussman SK (1998) Renal lymphoma: spectrum of CT findings and potential mimics. Am J Roentgenol 171:1067–1072

Sotelo-Avila C, Beckwith JB, Johnson JE (1995) Ossifying renal tumor of infancy: a clinicopathologic study of nine cases. Pediatr Pathol Lab Med 15:745–762

Vazquez JL, Barnewolt CE, Shamberger RC, Chung T, Perez-Atayde AR (1998) Ossifying renal tumor of infancy presenting as a palpable abdominal mass. Pediatr Radiol 28:454–457

Wesche WA, Wilimas J, Khare V, Parham DM (1998) Renal medullary carcinoma: a potential sickle cell nephropathy of children and adolescents. Pediatr Pathol Lab Med 18:97–113

White KS, Grossman H (1991) Wilms' and associated renal tumors of childhood. Pediatr Radiol 21:81–88